BIOCHEMISTRY
including biophysical chemistry & molecular biology

Article

pubs.acs.org/biochemistry

Structures of the Excited States of Phospholamban and Shifts in Their Populations upon Phosphorylation

Alfonso De Simone,[†,‡] Martin Gustavsson,[§] Rinaldo W. Montalvao,[‡] Lei Shi,[§] Gianluigi Veglia,[§,∥] and Michele Vendruscolo*[,‡]

[†]Division of Molecular Biosciences, Imperial College London, London SW7 2AZ, U.K.

[‡]Department of Chemistry, University of Cambridge, Cambridge CB2 1EW, U.K.

[§]Department of Biochemistry, Molecular Biology, and Biophysics, University of Minnesota, Minneapolis, Minnesota 55455, United States

[∥]Department of Chemistry, University of Minnesota, Minneapolis, Minnesota 55455, United States

Supporting Information

ABSTRACT: Phospholamban is an integral membrane protein that controls the calcium balance in cardiac muscle cells. As the function and regulation of this protein require the active involvement of low populated states in equilibrium with the native state, it is of great interest to acquire structural information about them. In this work, we calculate the conformations and populations of the ground state and the three main excited states of phospholamban by incorporating nuclear magnetic resonance residual dipolar couplings as replica-averaged structural restraints in molecular dynamics simulations. We then provide a description of the manner in which phosphorylation at Ser16 modulates the activity of the protein by increasing the sizes of the populations of its excited states. These results demonstrate that the approach that we describe provides a detailed characterization of the different states of phospholamban that determine the function and regulation of this membrane protein. We anticipate that the knowledge of conformational ensembles enable the design of new dominant negative mutants of phospholamban by modulating the relative populations of its conformational substates.

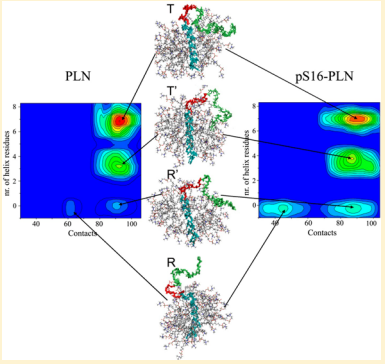

As proteins in solution undergo conformational fluctuations, in addition to the native structure they can populate other states with smaller populations and higher free energies.[1−13] These excited states are often important in enzymatic reactions and molecular recognition events, as they include the conformations that are selected by ligands or binding partners.[5−8] Nuclear magnetic resonance (NMR) spectroscopy can provide detailed information about such excited states at the atomic level.[4−7] For instance, structural properties of these states can be obtained by the analysis of resonance line widths or by nuclear spin relaxation measurements.[4,6,9,10] Another powerful approach exploits the introduction of partially aligned samples, which allows one to reintroduce anisotropy in the NMR observables and determine simultaneously the structure and dynamics of proteins.[14−17] The measurement of residual dipolar couplings (RDCs) makes it possible not only to characterize the ground states of the macromolecules but also to gain access to the structural features of excited states.[10,18] This approach was recently illustrated in the case of membrane proteins by the characterization of the pH-triggered activated-state conformations of the influenza hemagglutinin fusion peptide.[11]

In this work, we apply this strategy to an integral membrane protein and determine the structures of the ground and excited states of phospholamban (PLN). PLN is a type II membrane protein that in its unphosphorylated form binds and inhibits the sarcoplasmic reticulum Ca^{2+}-ATPase (SERCA).[19] PLN, which exists as a pentamer in the sarcoplasmic reticulum, disassembles into monomers to interact with SERCA.[19−21] When PLN is phosphorylated by protein kinase A (PKA) at Ser16, its inhibition is reversed, and the apparent Ca^{2+} affinity of SERCA increases without dissociation of the PLN−SERCA complex.[22,23] Dephosphorylation of PLN by protein phosphatase 1 ensures the cyclical regulation of this endogenous inhibitor.[19] PLN mutations are associated with the progression of heart failure.[24−26] Also, overexpression of a pseudophosphorylated form of PLN relieves the effect of heart failure in animal models by enhancing SERCA function, making the SERCA−PLN complex a promising therapeutic target[27,28]

Nuclear spin relaxation measurements revealed that PLN adopts an ensemble of conformations and identified four domains within the protein:[29,30] amphipathic α-helix domain Ia (residues 1−16), the loop region (residues 17−22), juxtamembrane domain Ib (residues 23−30), and transmembrane domain II (residues 31−52). Domains Ib and II form a continuous α-helix that crosses the bilayer toward the lumen at

Received: April 25, 2013
Revised: August 8, 2013
Published: August 22, 2013

   dx.doi.org/10.1021/bi400517b | *Biochemistry* 2013, 52, 6684−6694

about a 24° angle with respect to the bilayer normal.[31] This angle is reduced to about 11° in the pentameric form of PLN, which is believed to act as a storage state.[32,33] Domain Ia and the loop region face the cytoplasm. Studies conducted in membrane-mimicking systems indicated that there are four different conformational states for the cytoplasmic region of PLN:[34−37] the T state, in which domain Ia is associated with the membrane, the T′ state, which is membrane-associated with a partial unfolding of the α-helix in domain Ia, the R′ state, which is also membrane-associated but unfolded, and the R state, which is completely unfolded and dissociated from the membrane.[34−37]

The NMR structure of the T state of PLN in its monomeric form in dodecylphosphocholine (DPC) micelles was determined by using interatomic distance restraints from ^{15}N-edited nuclear Overhauser effect spectroscopy spectra, dihedral angle restraints from chemical shifts, and hydrogen bond information from H−D exchange factors.[38] These structures were further refined with RDC data, which were augmented with paramagnetic relaxation enhancement (PRE) measurements to reduce the degeneracy from the RDC solutions and remove the ambiguity in the translational degree of freedom between the solution and membrane domains.[39] The structure of the T state in DPC micelles is similar to that of the same state in lipid bilayers, which was determined by using a hybrid method in which solution NMR restraints were combined with solid-state NMR restraints.[40,41]

A growing body of evidence indicates that the R state plays a central role in determining the function of PLN, as this is the state selected by PKA for phosphorylation and the size of its population is increased upon interaction with SERCA.[36,42,43] More importantly, phosphorylation-induced relief of SERCA inhibition has been found to be directly correlated to an increase in the size of the population of excited (T′, R′, and R) states.[34,44,45] Therefore, PLN mutants with phosphomimetic mutations promoting the population of excited states are emerging as promising candidates for gene therapy.[28,46,47] As understanding the nature of the conformational equilibrium between the R and T states and the mechanism of the transition between them will help develop new therapeutic approaches to defective contractility cardiac disorders,[26,46] it is important to determine the structures of these excited states and to characterize their conformational fluctuations. Towards this goal, in this work we have defined the free energy landscape of PLN using an approach in which RDCs are used as replica-averaged structural restraints in molecular dynamics simulations.[48,49] In this approach, the RDCs are calculated during the simulations using a structure-based method[49] as averages over multiple replicas of the protein[48,49] to extract effectively the information about conformational fluctuations carried by the RDC data. Our results show that the cytoplasmic region of PLN, comprising domain Ia and the loop, explores a broad conformational space with four well-defined free energy minima, which correspond to the four states described in previous studies.[34−36] The analysis that we conducted further indicates that the statistical weights of these minima are shifted upon phosphorylation at Ser16 with a promotion of PLN to the excited states, in which domain Ia becomes more dynamic and unfolded.

MATERIALS AND METHODS

Sample Preparation. In this work, we used AFA-PLN, a functional monomeric variant of PLN, AFA-PLN, which has three mutations in the transmembrane helix (C36A, C41F, and C46A) was recombinantly expressed and purified from *Escherichia coli* as described previously.[50] A fourth mutation (S16E) was introduced by site-directed mutagenesis as described previously.[44] Phosphorylation at Ser16 was achieved by the recombinantly expressed catalytic subunit of PKA to a 1:2000 PKA:PLN ratio as previously described.[34,51] Acrylamide gels for RDC measurements were polymerized in glass tubes (5.7 mm inner diameter) from a mixture of 5.11% (w/v) acrylamide, 0.13% (w/v) bisacrylamide, 0.1% (w/v) ammonium persulfate, 0.0031% (w/v) TEMED, and 100 mM Tris-HCl (pH 8). For the polymerization of negatively charged gels, 25% of the acrylamide was substituted with 2-(acrylamido)-2-methyl-1-propanesulfonic acid (AMPS). The gels were washed twice in 50 mM NaH_2PO_4/Na_2HPO_4 buffer (pH 6.5) and twice in ddH_2O and subsequently cut into 10 mm pieces that were dehydrated at 42 °C for 16 h. NMR samples were prepared by reconstituting pS16-AFA-PLN into 100 mM dodecylphosphocholine (DPC) in buffer [6 M guanidinium hydrochloride (Gdn HCl), 20 mM $NaHPO_4$, 120 mM NaCl, and 0.01% NaN_3 (pH 6.0)] to a protein concentration of 0.5 mM. The Gdn HCl was subsequently removed by dialysis against the same buffer (without Gdn HCl). For anisotropic samples, a dried acrylamide gel was rehydrated with a protein sample for 16 h at 37 °C. A gel stretching apparatus (New Era Enterprises Inc.)[52] was used to transfer the gel into an open-ended NMR tube, leading the gel to stretch to ∼1.8 times its original length. The RDC data obtained for PLN weakly aligned in charged and uncharged gels are reported in Tables S1 and S2 of the Supporting Information. The two sets of RDCs are fairly independent, as indicated by their Q factor of 1.13 [root-mean-square deviation of 5.39 Hz (Figure S1 of the Supporting Information)].

NMR Experiments. NMR experiments were conducted at 310 K on a Varian Inova spectrometer operating at a proton frequency of 599.548 MHz. ^{15}N−^{1}H and ^{13}C′−^{15}N RDCs were measured as the difference in splitting between isotropic (no gel, J) and anisotropic (stretched gel, J + RDC) samples from two-dimensional TROSY-based experiments;[53] 1704 complex points were acquired in the direct ^{1}H dimension and 80 increments in the indirect ^{15}N dimension with spectral widths of 10000 and 1200 Hz for ^{1}H and ^{15}N, respectively. Zero-filling was performed to a final matrix size of 16384 × 8192 points. ^{13}C′−^{13}C$_\alpha$ couplings were measured from uncoupled three-dimensional HNCO experiments as the difference in J splitting between isotropic and anisotropic samples. Experiments were conducted with 1664 points in the direct ^{1}H dimension and 40 and 32 increments in the ^{13}C and ^{15}N dimensions, respectively. The spectral widths were 10000, 1000, and 1200 Hz for ^{1}H, ^{13}C, and ^{15}N, respectively. A recycle delay of 1.2 s was used for all experiments. All data were processed in NMRPipe and analyzed by Sparky.

Modeling of the PLN/DPC Micelle System. Molecular dynamics simulations with replica-averaged RDC restraints[48,49] (see below) were performed starting from one of the conformers of the NMR structural ensemble of PLN reconstituted in DPC micelles, which was previously obtained using nuclear Overhauser effects (NOEs), RDCs, and PRE restraints incorporated into a simulated annealing protocol using XPLOR-NIH.[39] The NOE and PRE data, however, were not used as restraints in the molecular dynamics simulations described in this work. One structure from this ensemble was inserted into an equilibrated DPC micelle with 60 lipid

dx.doi.org/10.1021/bi400517b | Biochemistry 2013, 52, 6684−6694

molecules; the overall results of the sampling, however, did not depend on the choice of the initial structure, as it should be expected at convergence. The initial coordinates of the DPC micelle were obtained from Wong.[54] The size of the DPC micelle (19.8 ± 1.9 Å) was chosen to match the size estimated by small-angle X-ray scattering measurements. The solvated DPC micelle was equilibrated for 0.5 ns before the insertion of PLN. A cylindrical space within the DPC micelle was created to accommodate the transmembrane domain of PLN. PLN and the DPC micelle were then brought together and subjected to minimization and equilibration.

Molecular dynamics simulations were conducted using a modified version of the GROMACS package[55] that implements RDCs as structural restraints[48,49,56] by using the Amber99SB force field[57] with improved parameters for the backbone[58] and side chains.[59] DPC parameters were derived by Tieleman et al.[60] The system composed by PLN in a DPC micelle was inserted in a cubic box with starting dimensions of 70 Å × 70 Å × 70 Å and solvated with 9298 explicit TIP3P water molecules.[61] Bonds were constrained by the LINCS algorithm.[62] The particle mesh Ewald (PME) method[63] was used to account for the electrostatic contributions to nonbonded interactions with a grid spacing of 0.12 nm. The protonation states of pH-sensitive residues were set as follows: Arg and Lys as positively charged, Asp and Glu as negatively charged, and His as neutral. The net charge of the system was neutralized by the addition of Cl^- and Na^+ ions. The system was equilibrated with external temperature and pressure baths (*NPT* ensemble) by using the v-rescale[64] and Berendsen[65] algorithms, respectively, and coupling time steps of 0.1 and 1.0 ps, respectively.

Molecular Dynamics Simulations with Replica-Averaged RDC Restraints. The use of NMR parameters as replica-averaged structural restraints in molecular dynamics simulations offers the possibility of interpreting the experimental measurements in terms of the maximum entropy principle[66−68] and, therefore, in the case presented here, to translate the RDC measurements into structural ensembles that represent the Boltzmann distributions of PLN and pS16-PLN. In this approach, the force field used in the molecular dynamics simulations is modified through the incorporation of the experimental information to modify the force field in the minimal manner that allows one to eliminate almost completely the deviations from the experimental data used in the simulations.[66−68]

Molecular dynamics simulations with replica-averaged RDC restraints were performed to determine the structural ensembles of PLN and pS16-PLN by adopting a structure-based calculation of the alignment tensor that accounted for the interaction between the PLN/micelle system and the alignment media.[48,49]

In the approach that we used, the RDC restraints are imposed by adding a pseudoenergy term (E^{RDC}) to a standard molecular mechanics force field (E^{FF})

$$E^{total} = E^{FF} + E^{RDC} \quad (1)$$

The resulting force field (E^{total}) is employed in molecular dynamics simulations, where the pseudoenergy term is given by

$$E^{RDC} = \alpha \sum_i (D_i^{res} - D_i^{ref})^2 \quad (2)$$

The restraints are imposed as averages over 16 replicas of the system.[48,49] Although the maximum entropy principle justification for the use of replica-averaged restraints in principle holds for an infinitely large number of replicas,[66,68] in practice excellent results have already been obtained for relatively small numbers such as those used here.[48,49,66,68] From previous studies, we estimate that the errors in the determination of the populations should be below 4%.[48,49] We also note that the number of replicas should be chosen according to arguments such as the convergence of the Shannon entropy (see, e.g., Figure 2 of ref 66), and is independent from the number of free energy minima of the system under investigation. For each replica, the alignment tensor is independently computed.[48,49] To save computational time, the tensors are computed individually on each replica every 250 steps, as they do not vary significantly over shorter intervals.[48,49] An initial equilibration simulation at 310 K (the temperature at which PLN is active in its physiological environment, which is also the temperature at which the RDCs were recorded[39]) was run, during which the agreement between calculated and experimental RDCs was allowed to converge by progressively increasing the weight α of the restraints. Subsequently, a series of 50 cycles of simulated annealing between 310 and 500 K were conducted to sample the region of conformational space compatible with the RDC restraints. Each annealing cycle was conducted for a total of 8 ns (500 ps per replica) by using an integration step of 1 fs. After equilibration at 310 K, the final 100 ps of each annealing cycle was used to compute the equilibrated ensemble of 9600 structures by sampling the conformers from each replica every 5 ps. The initial 20 cycles were discarded from the analyses. During each cycle, typically each replica explores (with different frequencies) the four minima on the free energy landscape.

The molecular dynamics trajectories for both PLN and pS16-PLN were generated by employing as structural restraints the RDC data measured in neutral gels (Figure 1), while those measured in charged gels were used for validation. The conformations of PLN in charged and uncharged gels are virtually identical, as illustrated by the overlay of the protein $^1H-^{15}N$ HSQC spectra in the two alignment media (Figure S2 of the Supporting Information).

As the approach that we used in this work was previously used only for globular proteins,[48,49] to test its robustness in the case of membrane proteins solubilized in detergent micelles, we applied it to DsbB, a multispan membrane protein reconstituted in DPC micelles and aligned in positively charged gels.[69] By using the available RDCs[69] as replica-averaged structural restraints as described above, we found that the native state of DsbB that we determined is characterized by conformational fluctuations with an amplitude smaller than that of PLN (Figure S3A of the Supporting Information) and an overall remarkable agreement between experimental and calculated RDC values (Figure S3 of the Supporting Information).

RESULTS AND DISCUSSION

Substate Structure Determination. In the free energy landscape view of protein behavior, native states of proteins may often involve an equilibrium between different substates in rapid conformational exchange.[1−13] In these cases, the NMR measurement of an observable D reports on the average value of the observable across N substates

$$D = \sum_k p_k D_k \quad (3)$$

dx.doi.org/10.1021/bi400517b | Biochemistry 2013, 52, 6684−6694

where k runs over the N substates, which have populations p_k and values D_k of the observable D. In the case of a single substate ($N = 1$), eq 3 corresponds to the standard structure determination problem, in which one determines the structure of a protein given a set of experimental data. More generally, however, the number of substates (N) is not known in advance and should also be determined from the data.

A question of great interest is whether, in the presence of multiple substates, given only the average value D one can determine the number of substates, their structures, and the values of their populations. Although in principle a solution of this problem must exist, which corresponds to the true N, p_k, and D_k values, it remains to be established under which conditions, if at all, one can overcome the degeneracy of the solution, as multiple sets of N, p_k, and D_k values may correspond to a given D in eq 3.

The initial evidence that, at least in the case of two substates ($N = 2$), there are approaches that can identify nondegenerate solutions was provided in a study in which two conformational substates of ribonuclease A were determined simultaneously from RDC data,[56] and from chemical shift data.[70] These results were obtained by using the NMR data as replica-averaged structural restraints in molecular dynamics simulations, as this procedure represents an optimal way to generate structural ensembles according to the maximum entropy principle (66−68), which in practice means that given a force field and a set of experimental data, this procedure results in an ensemble of conformations most compatible with both the force field and the experimental data, without making any further assumption.

To validate the results, in favorable cases, one can measure directly the NMR parameters of the substates, i.e., the D_k values, and thus verify directly whether the substate structure determination procedure has been conducted correctly. A most powerful approach to achieve this result is to use relaxation dispersion methods, which have been used to determine directly the structures of excited states of proteins with small populations that exchange on the millisecond time scale with the most populated state.[4,9,10] It should also be noted that a very important validation is represented by the value of N, because this value may be known experimentally through a variety of means. If the procedure results in a value of N consistent with independent observations, one has at least an initial indication of the validity of the calculations.

In this work, we apply the substate structure determination approach to find the substates of phospholamban using residual dipolar couplings as replica-averaged structural restraints in molecular dynamics simulations, as this procedure may represent an effective implementation for solving the substate structure determination problem.

Residual Dipolar Couplings of PLN and pS16-PLN. We studied the conformational properties of PLN in the monomeric state, which was stabilized by mutating three transmembrane Cys residues (C36A, C41F, and C46A);[71] the resulting mutational variant has an activity nearly identical to that of wild-type PLN.[71] Relaxation measurements of PLN identified four domains with different backbone dynamics.[29] These four domains also reflect specific patterns in the $^{15}N-^{1}H$ RDC profiles with the region spanning domain Ia exhibiting positive RDC values with an average of 2.14 Hz and a standard deviation of 3.00 Hz, whereas the flexible region covering the loop and domain Ib presents slightly negative RDC values with an average of −1.16 Hz and a standard deviation of 4.31 Hz[39] (Figure 1). A different RDC pattern is associated with

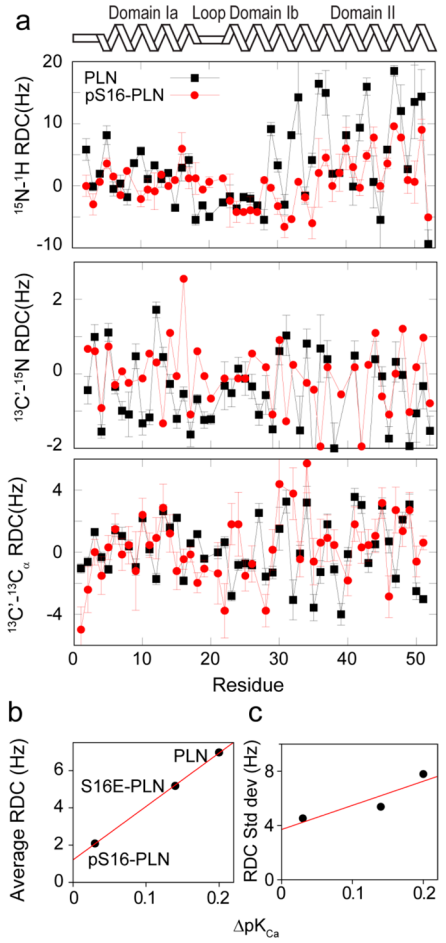

Figure 1. (a) Comparison of the residual dipolar couplings of PLN (black) and pS16-PLN (red) measured in stretched polyacrylamide gels. (b) Correlation between the average RDCs of domain II and the PLN-induced inhibition of SERCA, as assessed by the ΔpK_{Ca} values[34] (see Materials and Methods) for PLN, pS16-PLN, and S16E-PLN. (c) Correlation between the standard deviations of the RDCs of domain II and the PLN-induced inhibition of SERCA, assessed as described for panel b.

membrane-spanning domain II, which shows stronger positive RDC values with an average of 6.52 Hz and a standard deviation of 7.90 Hz[39] (Figure 1). The errors in the $^{15}N-^{1}H$ RDCs were determined as the standard error of three measurements using three separate sample preparations. For the $^{13}C'-^{15}N$ and $^{13}C'-^{13}C_\alpha$ RDCs, the errors were estimated as

$$\Delta D = \sqrt{\left(\frac{\Delta\upsilon_{ani}}{\sigma_{ani}}\right)^2 + \left(\frac{\Delta\upsilon_{iso}}{\sigma_{iso}}\right)^2} \quad (4)$$

where $\Delta\upsilon_{ani}$ and $\Delta\upsilon_{iso}$ are the anisotropic (in stretched gels) and isotropic (with no gels) line widths, respectively, and σ_{ani} and σ_{iso} are the anisotropic and isotropic signal-to-noise ratios, respectively.

RDC measurements of a phosphorylated form of PLN (pS16-PLN) show significant variations within domain II with a substantial reduction in the average and standard deviation [2.46 and 5.49 Hz, respectively (Figure 1)]. These findings indicate that phosphorylation of Ser16 has strong effects on the structure and dynamics of PLN, which is consistent with previous studies.[51] Because Ser16 phosphorylation does not

dx.doi.org/10.1021/bi400517b | Biochemistry 2013, 52, 6684−6694

affect the dynamics of domain II, the reduced intensities of $^{15}N-^{1}H$ RDCs are likely to arise from an increased degree of dispersion of the mutual orientations of the dynamic domains of PLN.

It has also been previously established that the pseudophosphorylation of PLN at Ser16, as realized by the S16E mutation, leads to a partial loss of SERCA inhibition.[34] Consistently, the RDCs for the S16E mutant are intermediate between those of PLN and pS16-PLN (Figure 1b), with an average and a standard deviation in domain II of 5.18 and 5.38 Hz, respectively (Figure 1b,c). The approximately linear correlation between RDCs and inhibitory function (Figure 1b), which was measured by the ΔpK_{Ca} values[34] (determined as $pK_{CaSERCA} - pK_{CaSERCA+PLN}$), provides further support for the view that the RDCs are sensitive to structural fluctuations that are integral to PLN function.

Determination of the Structures of the Four Substates of PLN. To account for the conformational fluctuations of PLN, RDCs corresponding to $^{15}N-^{1}H$, $^{13}C'-^{15}N$, and $^{13}C'-^{13}C\alpha$ bond vectors were used as replica-averaged structural restraints in molecular dynamics simulations[48,49] to determine a structural ensemble of this protein (see Materials and Methods). The calculations were started from a structure previously determined by NOEs, RDCs, and PREs[39] (Figure 2a), although the NOEs and PREs were not used as restraints in the calculations described here.

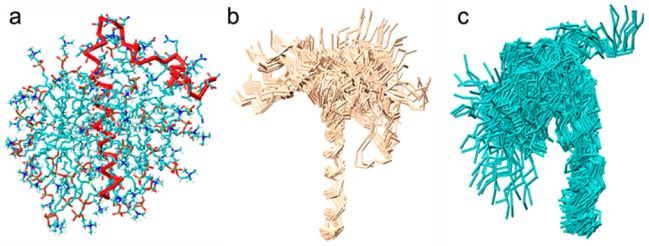

Figure 2. Structural ensembles of PLN and pS16-PLN. (a) Starting model of PLN in a DPC micelle. (b) Ensemble of conformations of PLN. (c) Ensemble of conformations of pS16-PLN.

Several methods have been proposed to exploit the information provided by RDC measurements to characterize the dynamics of proteins.[49,56,72−78] Although the majority of these approaches have been used to assess conformational fluctuations of a relatively small amplitude, we have recently shown that RDCs can be employed to describe large-scale structural dynamics like those associated with the functional fluctuations of enzymes.[48,49] The method that we used is based on the treatment of RDCs as replica-averaged restraints in molecular dynamics simulations in which the RDCs are calculated from the shape and charge of each individual structure in the ensemble.[79] By using this method, we have shown that it is possible to reproduce the conformational equilibria among different states populated by proteins.[48,49]

The structural ensemble of PLN that we obtained was determined by enforcing an agreement between experimental and back-calculated RDC values (Figure S4 of the Supporting Information), resulting in Q factors of 0.12, 0.16, and 0.16 for $^{15}N-^{1}H$, $^{13}C'-^{15}N$, and $^{13}C'-^{13}C\alpha$ bond vectors, respectively. To validate this ensemble, we used it to back-calculate the values of NMR parameters that were not used as restraints in the structure calculations. First, we used RDC data recorded in negatively charged acrylamide/bisacrylamide gels (Figure S5A,B of the Supporting Information); these data were not employed as restraints in the calculations, thereby providing an independent assessment of the quality of the structures obtained. By using a structure-based alignment method to back-calculate the RDC values[48,49] (see Materials and Methods), the ensemble results in an excellent agreement with charged gel RDC values. We found, however, a poorer agreement when we employed an alternative method based on the fitting of the experimental RDC values to the structures [the SVD method[80] (Figure S6 of the Supporting Information)]. These findings underscore the importance of using a structure-based method of alignment in the presence of large conformational fluctuations of proteins. In the structure-based approach that we followed[48,49] (see Materials and Methods), none of the structures of the ensemble is required to match individually the experimental data, because the values of the latter are averaged over a heterogeneous ensemble of structural states and cannot be attributed to a single conformation.[48,49] By contrast, in the SVD method, the alignment tensor of individual conformations is fitted by requiring an optimal match with the RDC data, a procedure that may not be very accurate if the RDC data themselves refer to an ensemble of structurally different conformations.[48] The calculations conducted by applying the RDC restraints to single conformations resulted in poorer agreement with the RDC measurements (Figure S7 of the Supporting Information). Further validation of the structural ensemble that we determined was obtained by comparing experimental and back-calculated chemical shifts, which resulted in a very good agreement (Figure S5c of the Supporting Information).

One of the main characteristics of the structural ensemble that we determined is the presence of a well-defined C-terminal α-helical domain in the hydrophobic region of the micelle. This α-helix, which exhibits an average root-mean-square fluctuation of 1 Å on the Cα atoms, does not resemble the curved shape that was reported previously for pentameric PLN[81] but is in agreement with the conformation of the same pentameric PLN derived from solid-state NMR measurement in lipid bilayers[32] and from NOEs, RDCs, and PREs[39] for the AFA-PLN monomer in micelles. This difference arises because of the averaging procedure that we used in this work, which accounts for the conformational fluctuations of PLN without assuming the presence of a well-defined average structure of the entire molecule (Figure 1b). The structures that we obtained indicate that the N-terminal region of PLN is highly heterogeneous and assumes a large variety of orientations on the micelle surface compared to the C-terminal α-helical frame (Figure 1b). The analysis of the structural ensemble shows that C-terminal domain II adopts a stable α-helical conformation (Figure 3a), while N-terminal domain Ia adopts a less populated α-helical conformation with parameters that deviate from the canonical α-helical parameters (Figure 3a).

Validation of the Structures of PLN Using Chemical Shifts. The α-helical features described above are in good agreement with the conformational analysis conducted with δ2D,[82] which employs chemical shifts for an accurate determination of secondary structure populations (Figure 3b). The correspondence between the results obtained independently using either RDC information (Figure 3a) or chemical shift information (Figure 3b) about the α-helical features of PLN provides support for the validity of the conformations that we determined for PLN.

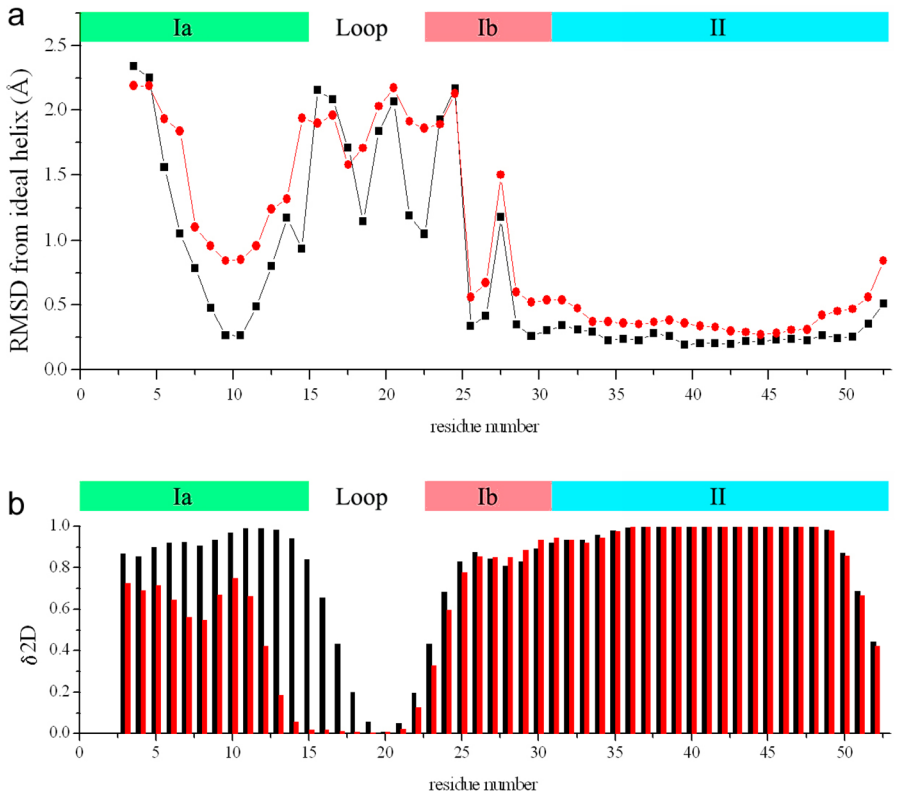

Figure 3. Comparison of the residue-specific α-helical populations of PLN and pS16-PLN. Black and red symbols denote data for PLN and pS16-PLN, respectively. The location of the four domains of PLN is indicated in the top of each panel. (a) Local root-mean-square deviation (rmsd) from an ideal α-helix. The rmsd is calculated by using a running four-residue window. The rmsd of the window is assigned to the average position of the residues. (b) α-Helix populations calculated by using δ2D,[82] by employing the measured chemical shifts of PLN and pS16-PLN. The errors in the per-residue populations estimated with the δ2D method have been reported to be below 8%.[82]

As the structures of the four substates of PLN that we have determined were obtained using RDC values averaged over all of them (see eq 3), a stringent validation would be provided by comparing the structures with independent experimental data measured specifically for the individual substates. As these substates, however, are in fast exchange, it is very challenging to perform such measurements. We have therefore exploited the observation that the population of the R state can be progressively increased by altering the sequence of PLN, either by mutations or by truncations. In particular, we compare here the chemical shifts back-calculated for the T and R states, which were calculated as averages over all the conformations of the two states, and those experimentally measured for a peptide corresponding to the cytoplasmic domain of PLN, which is unstructured.[42] The results indicate that the cytoplasmic domain in the R state has chemical shifts intermediate between those of the T state, which is ordered, and an unstructured state (Figure 4).

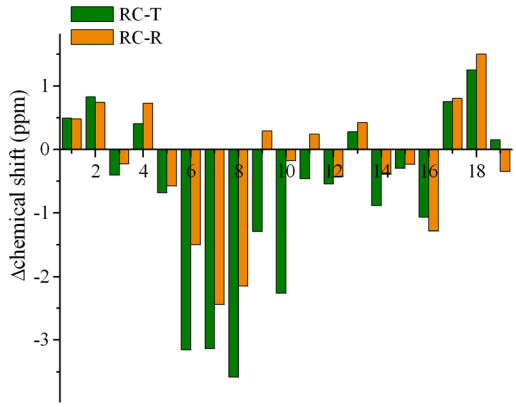

Figure 4. Comparison of the chemical shifts back-calculated from the structures of the T and R states with those experimentally measured[42] for an unstructured peptide corresponding to the cytoplasmic domain of PLN. The analysis of the differences between the chemical shifts of the T state and the peptide (green) and between the R state and the peptide (orange) indicates that the R state exhibits a degree of structural order intermediate between that of the T state and that of the unstructured peptide.

Effect of Phosphorylation on the Conformational Properties of PLN. To characterize the structural effects of phosphorylation of Ser16 on the backbone dynamics of PLN, we repeated the structure calculations using RDCs measured on the pS16-PLN variant. The resulting ensemble of conformations had Q factors of 0.09, 0.10, and 0.11 for ^{15}N−^{1}H, ^{13}C′−^{15}N, and ^{13}C′−^{13}Cα, respectively. Very good agreement is also found for the validation of the ensemble with independent data of RDCs measured in charged gels and chemical shifts (Figure S5 of the Supporting Information). The calculations were performed by using the same protocol that was employed for PLN, but with a phosphoserine at position 16.

Our findings indicate that pS16-PLN exhibits conformational fluctuations that are larger in amplitude than those of PLN. The amplitude of these fluctuations significantly increases in particular in the C-terminal α-helix (domain II) with an average root-mean-square fluctuation of 2.24 Å (Figure 3). The

dx.doi.org/10.1021/bi400517b | Biochemistry 2013, 52, 6684−6694

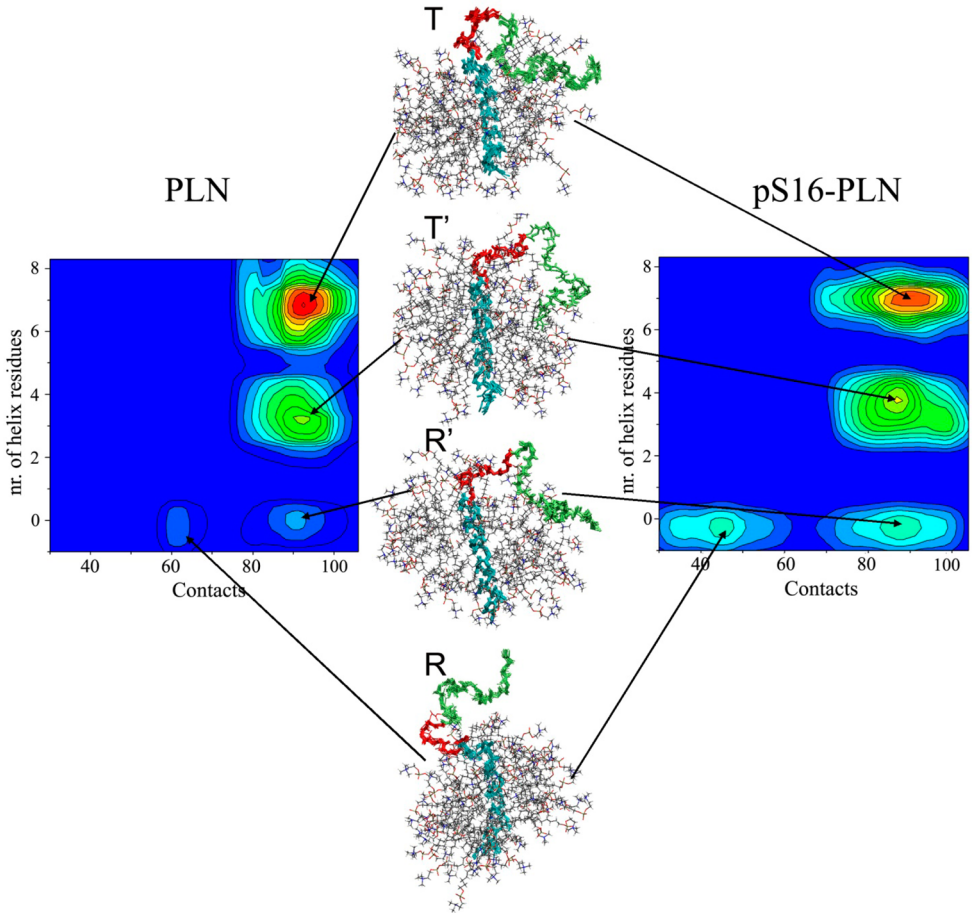

Figure 5. Comparison of the free energy landscapes of PLN and pS16-PLN. The free energy is given as a function of the number of contacts among backbone atoms of the N-terminal region of the protein (residues 1−30) and DPC molecules and of the number of α-helical residues in domains Ia and Ib. Upon phosphorylation at Ser16, the sizes of the populations of the R and R′ states increase. A representative structure of the R state has been deposited in the Protein Data Bank as entry 2LPF.

orientations of the N-terminal domain compared to the C-terminal domain are significantly more dispersed than in the PLN ensemble (Figure 2c), with a decrease in the α-helical content of the N-terminal helix (domain Ia), which is now populated at 40% (Figure 3). Hence, the structural ensemble of pS16-PLN suggests that phosphorylation at Ser16 dramatically alters the conformational fluctuations of PLN and destabilizes the secondary structure elements.

Free Energy Landscapes of PLN and pS16-PLN. By projecting the structural ensembles onto specific order parameters, we identified the main features of the free energy landscapes of PLN and pS16-PLN. We choose two order parameters that account for independent characteristics of the PLN ensembles. As the present study is aimed at the characterization of structural states connected to folding and unfolding events of PLN, as well as its adsorption and detachment from the surface of micelles, we chose as reaction coordinates the number of residues in α-helical conformations at the N-terminus (domains Ia and Ib) and the number of contacts between the N-terminal region of the protein (residues 1−30) and the micelle (Figure 5). These coordinates were chosen because they report on the most relevant conformational features that distinguish the R and T states. This projection identifies four structural forms closely resembling the four PLN states previously proposed on the basis of chemical shift analysis and EPR methods[34] and provides molecular details of these low populated conformational states that are crucial for PLN function.

The most populated free energy basin of the PLN ensemble presents an α-helical structure in domains Ia and Ib and a large number of contacts with the micelle surface (Figure 5); this state exhibits the structural features of the T state of PLN. A second basin, corresponding to the T′ state, presents a large number of contacts with the micelle but a reduced α-helical content (Figure 5). A minor basin, R′, still presents a large fraction of contacts with the micelle but lacks any persistent secondary structure element within domains Ia and Ib (Figure 5). Such an unfolded state corresponds to the R′ state as previously hypothesized on the basis of chemical shift analysis.[34] Finally, a low populated state in PLN does not show secondary structure formation in the N-terminal region of the protein and has a reduced number of contacts with the micelle. This conformation represents an excited state, the R state, in which the N-terminus of the protein is unfolded and exposed to the bulk solvent (Figure 5).

We also repeated the molecular dynamics simulations described above without RDC restraints. This procedure resulted in very different free energy landscapes exhibiting only two substates (Figure S8 of the Supporting Information). Therefore, this procedure would give $N = 2$ in eq 3 instead of $N = 4$, which is known independently to be the case.[34−37] These results demonstrate that the appearance of the T′, R′, and R

dx.doi.org/10.1021/bi400517b | *Biochemistry* 2013, 52, 6684−6694

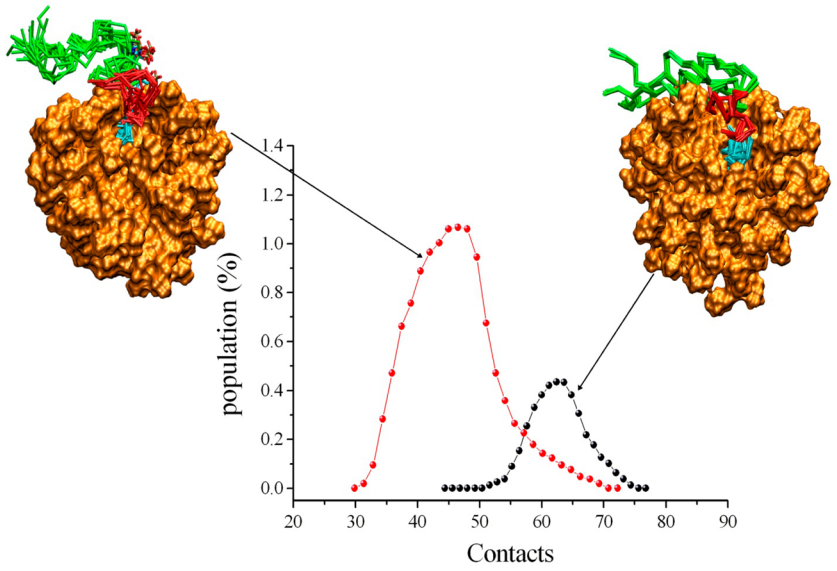

Figure 6. Comparison of the R states of PLN and pS16-PLN. The R state is nearly 3-fold more populated in pS16-PLN (red curve) than in PLN (black curve) and is characterized by a smaller number of contacts between the cytoplasmic residues (domain Ia, loop, and domain Ib) and the micelle surface.

states of PLN is not a consequence of the force field used in the molecular dynamics simulations, but of the replica-averaged RDC restraints added to the force field itself. We conclude that our method samples the different conformational states of proteins and that the procedure that we followed is capable of reproducing statistical weights of metastable states and conformational equilibria in proteins.[48,49]

We then repeated the analysis for pS16-PLN. Our results indicate that phosphorylation of Ser16 induces a redistribution of the Boltzmann weights of the four states of PLN (Figure 5). We found that the T state of pS16-PLN has a lower population (37%) than the unphosphorylated form (55%) and that the R′ and R states have significantly higher populations (from 7 to 13% and from 4 to 12%, respectively). The result that the R state trebles the size of its population upon phosphorylation is consistent with previous NMR[34] and EPR[36] results. Also, the increase in the population of the excited state is directly correlated to the loss of inhibitory function upon phosphorylation.[34,36,44] The reduction in the number of contacts for the R state is more pronounced for pS16-PLN, indicating a stronger tendency of the N-terminal region to detach from the micelle surface (Figure 6). This finding could arise from charge repulsion introduced upon phosphorylation.

In summary, we identified four structural states in a conformational equilibrium within the heterogeneous ensemble of PLN in the presence of micelles, thus providing information about the structural features of the states that are crucial for the biological activity of PLN, although in the presence of lipid bilayers some details, in particular the populations of the different states, may be expected to be different. In this context, the redistribution of the populations of these four states upon phosphorylation illustrates the type of conformational equilibria that dictate the biological properties of this protein.

CONCLUSIONS

The conformational equilibria between the different states of PLN are particularly relevant for determining the biological function of this protein. In the absence of a membrane, the cytoplasmic domains of PLN remain intrinsically disordered, while membranes and membrane-mimicking systems induce them to form more ordered states (the T and T′ states). The various conformational states of PLN have different activities, as indicated by biochemical assays and NMR and EPR studies, which suggest that the conformational fluctuations of PLN have a prominent role in the regulation of the activity of SERCA. Through these fluctuations, PLN occupies more disordered states (R and R′), whose characterization at the atomic level has been very challenging because of their low populations. In this study, we have demonstrated that the incorporation of residual dipolar couplings as replica-averaged structural restraints in molecular dynamics simulations provides an accurate free energy landscape of PLN and enables one to characterize the four basins corresponding to the T, T′, R, and R′ states, which were previously identified by chemical shift trajectories in unfolding experiments,[34] and to determine the corresponding conformations at atomic-level resolution.

These results open the possibility of correlating the population levels of the excited states of PLN with the biological function of this protein. We have recently shown that populating the R state is a condition for PLN to be selected by protein kinase A for phosphorylation.[42] When the equilibrium is shifted toward the T state, the phosphorylation efficiency decreases dramatically, whereas an increase in the population of the R state increases the rate of phosphorylation of Ser16. Because the cytoplasmic domain of PLN interacts with at least seven different partners,[19] we anticipate that these proteins may select and bind different members in the structural ensemble of PLN.

The results that we have presented suggest novel opportunities for the identification of novel loss-of-function (dominant-negative) PLN analogues, which have been proposed as a possible therapeutic strategy for defective contractility cardiac disorders.[26,46] Support for this view has been provided recently by the demonstration that it is possible to tune the conformational fluctuations of PLN to regulate the function of SERCA and in turn muscle contractility.[34,44] An increase in the size of the population of the R state of PLN by site-specific mutations localized in the dynamic loop or using

dx.doi.org/10.1021/bi400517b | *Biochemistry* 2013, 52, 6684−6694

the phosphomimetic mutation S16E was shown to lead to an enhancement of the apparent Ca^{2+} affinity of SERCA, with significant benefits for cardiac contractility.[27] We anticipate that the availability of the structures of the excited states of PLN determined in this work will help in the creation of even more effective dominant-negative mutants and identification of small molecules capable of regulating the conformational equilibria of PLN.

■ ASSOCIATED CONTENT

Supporting Information

Figures S1−S8 and Tables S1 and S2. This material is available free of charge via the Internet at http://pubs.acs.org.

■ AUTHOR INFORMATION

Corresponding Author

*E-mail: mv245@cam.ac.uk. Phone: +44 1223 763873.

Funding

This work was supported by grants from EPSRC (A.D.S.), EMBO (A.D.S.), Marie Curie (A.D.S.), BBSRC (R.W.M. and M.V.), and the National Institutes of Health (GM64742 to G.V.).

Notes

The authors declare no competing financial interest.

■ REFERENCES

(1) Frauenfelder, H., Sligar, S. G., and Wolynes, P. G. (1991) The energy landscapes and motions of proteins. *Science 254*, 1598−1603.

(2) Dobson, C. M. (2003) Protein folding and misfolding. *Nature 426*, 884−890.

(3) Karplus, M., and Kuriyan, J. (2005) Molecular dynamics and protein function. *Proc. Natl. Acad. Sci. U.S.A. 102*, 6679−6685.

(4) Neudecker, P., Robustelli, P., Cavalli, A., Walsh, P., Lundstrom, P., Zarrine-Afsar, A., Sharpe, S., Vendruscolo, M., and Kay, L. E. (2012) Structure of an intermediate state in protein folding and aggregation. *Science 336*, 362−366.

(5) Boehr, D. D., Nussinov, R., and Wright, P. E. (2009) The role of dynamic conformational ensembles in biomolecular recognition. *Nat. Chem. Biol. 5*, 789−796.

(6) Baldwin, A. J., and Kay, L. E. (2009) NMR spectroscopy brings invisible protein states into focus. *Nat. Chem. Biol. 5*, 808−814.

(7) Kalodimos, C. G. (2011) NMR reveals novel mechanisms of protein activity regulation. *Protein Sci. 20*, 773−782.

(8) Vendruscolo, M. (2011) Excited-state control of protein activity. *J. Mol. Biol. 412*, 153−154.

(9) Bouvignies, G., Vallurupalli, P., Hansen, D. F., Correia, B. E., Lange, O., Bah, A., Vernon, R. M., Dahlquist, F. W., Baker, D., and Kay, L. E. (2011) Solution structure of a minor and transiently formed state of a T4 lysozyme mutant. *Nature 477*, 111−114.

(10) Korzhnev, D. M., Religa, T. L., Banachewicz, W., Fersht, A. R., and Kay, L. E. (2010) A transient and low-populated protein-folding intermediate at atomic resolution. *Science 329*, 1312−1316.

(11) Lorieau, J. L., Louis, J. M., Schwieters, C. D., and Bax, A. (2012) pH-triggered, activated-state conformations of the influenza hemagglutinin fusion peptide revealed by NMR. *Proc. Natl. Acad. Sci. U.S.A. 109*, 19994−19999.

(12) Marsh, J. A., Teichmann, S. A., and Forman-Kay, J. D. (2012) Probing the diverse landscape of protein flexibility and binding. *Curr. Opin. Struct. Biol. 22*, 643−650.

(13) Guerry, P., Salmon, L., Mollica, L., Roldan, J. L. O., Markwick, P., van Nuland, N. A. J., McCammon, J. A., and Blackledge, M. (2013) Mapping the population of protein conformational energy sub-states from NMR dipolar couplings. *Angew. Chem., Int. Ed. 52*, 3181−3185.

(14) Tjandra, N., and Bax, A. (1997) Direct measurement of distances and angles in biomolecules by NMR in a dilute liquid crystalline medium. *Science 278*, 1111−1114.

(15) Tolman, J. R., Flanagan, J. M., Kennedy, M. A., and Prestegard, J. H. (1997) NMR evidence for slow collective motions in cyanometmyoglobin. *Nat. Struct. Biol. 4*, 292−297.

(16) Bax, A. (2003) Weak alignment offers new NMR opportunities to study protein structure and dynamics. *Protein Sci. 12*, 1−16.

(17) Blackledge, M. (2005) Recent progress in the study of biomolecular structure and dynamics in solution from residual dipolar couplings. *Prog. Nucl. Magn. Reson. Spectrosc. 46*, 23−61.

(18) Vallurupalli, P., Hansen, D. F., and Kay, L. E. (2008) Structures of invisible, excited protein states by relaxation dispersion NMR spectroscopy. *Proc. Natl. Acad. Sci. U.S.A. 105*, 11766−11771.

(19) MacLennan, D. H., and Kranias, E. G. (2003) Phospholamban: A crucial regulator of cardiac contractility. *Nat. Rev. Mol. Cell Biol. 4*, 566−577.

(20) Cornea, R. L., Autry, J. M., Chen, Z. H., and Jones, L. R. (2000) Reexamination of the role of the leucine/isoleucine zipper residues of phospholamban in inhibition of the Ca^{2+} pump of cardiac sarcoplasmic reticulum. *J. Biol. Chem. 275*, 41487−41494.

(21) Cornea, R. L., Jones, L. R., Autry, J. M., and Thomas, D. D. (1997) Mutation and phosphorylation change the oligomeric structure of phospholamban in lipid bilayers. *Biochemistry 36*, 2960−2967.

(22) Wegener, A. D., Simmerman, H. K. B., Lindemann, J. P., and Jones, L. R. (1989) Phospholamban phosphorylation in intact ventricles: Phosphorylation of serine-16 and threonine-17 in response to β-adrenergic stimulation. *J. Biol. Chem. 264*, 11468−11474.

(23) James, Z. M., McCaffrey, J. E., Torgersen, K. D., Karim, C. B., and Thomas, D. D. (2012) Protein-protein interactions in calcium transport regulation probed by saturation transfer electron paramagnetic resonance. *Biophys. J. 103*, 1370−1378.

(24) Schmitt, J. P., Kamisago, M., Asahi, M., Li, G. H., Ahmad, F., Mende, U., Kranias, E. G., MacLennan, D. H., Seidman, J. G., and Seidman, C. E. (2003) Dilated cardiomyopathy and heart failure caused by a mutation in phospholamban. *Science 299*, 1410−1413.

(25) Haghighi, K., Kolokathis, F., Gramolini, A. O., Waggoner, J. R., Pater, L., Lynch, R. A., Fan, G. C., Tsiapras, D., Parekh, R. R., Dorn, G. W., MacLennan, D. H., Kremastinos, D. T., and Kranias, E. G. (2006) A mutation in the human phospholamban gene, deleting arginine 14, results in lethal, hereditary cardiomyopathy. *Proc. Natl. Acad. Sci. U.S.A. 103*, 1388−1393.

(26) Haghighi, K., Kolokathis, F., Pater, L., Lynch, R. A., Asahi, M., Gramolini, A. O., Fan, G. C., Tsiapras, D., Hahn, H. S., Adamopoulos, S., Liggett, S. B., Dorn, G. W., MacLennan, D. H., Kremastinos, D. T., and Kranias, E. G. (2003) Human phospholamban null results in lethal dilated cardiomyopathy revealing a critical difference between mouse and human. *J. Clin. Invest. 111*, 869−876.

(27) Hoshijima, M., Ikeda, Y., Iwanaga, Y., Minamisawa, S., Date, M. O., Gu, Y. S., Iwatate, M., Li, M. X., Wang, L. L., Wilson, J. M., Wang, Y. B., Ross, J., and Chien, K. R. (2002) Chronic suppression of heart-failure progression by a pseudophosphorylated mutant of phospholamban via in vivo cardiac raav gene delivery. *Nat. Med. 8*, 864−871.

(28) Kho, C., Lee, A., and Hajjar, R. J. (2012) Altered sarcoplasmic reticulum calcium cycling-targets for heart failure therapy. *Nat. Rev. Cardiol. 9*, 717−733.

(29) Metcalfe, E. E., Zamoon, J., Thomas, D. D., and Veglia, G. (2004) H-1/N-15 heteronuclear NMR spectroscopy shows four dynamic domains for phospholamban reconstituted in dodecylphosphocholine micelles. *Biophys. J. 87*, 1205−1214.

(30) Traaseth, N. J., and Veglia, G. (2010) Probing excited states and activation energy for the integral membrane protein phospholamban by NMR CPMG relaxation dispersion experiments. *Biochim. Biophys. Acta 1798*, 77−81.

(31) Traaseth, N. J., Buffy, J. J., Zamoon, J., and Veglia, G. (2006) Structural dynamics and topology of phospholamban in oriented lipid bilayers using multidimensional solid-state NMR. *Biochemistry 45*, 13827−13834.

(32) Verardi, R., Shi, L., Traaseth, N. J., Walsh, N., and Veglia, G. (2011) Structural topology of phospholamban pentamer in lipid bilayers by a hybrid solution and solid-state NMR method. *Proc. Natl. Acad. Sci. U.S.A. 108*, 9101−9106.

(33) Becucci, L., Cembran, A., Karim, C. B., Thomas, D. D., Guidelli, R., Gao, J. L., and Veglia, G. (2009) On the function of pentameric phospholamban: Ion channel or storage form? *Biophys. J. 96*, L60−L62.
(34) Gustavsson, M., Traaseth, N. J., Karim, C. B., Lockamy, E. L., Thomas, D. D., and Veglia, G. (2011) Lipid-mediated folding/unfolding of phospholamban as a regulatory mechanism for the sarcoplasmic reticulum Ca^{2+}-ATPase. *J. Mol. Biol. 408*, 755−765.
(35) Karim, C. B., Kirby, T. L., Zhang, Z. W., Nesmelov, Y., and Thomas, D. D. (2004) Phospholamban structural dynamics in lipid bilayers probed by a spin label rigidly coupled to the peptide backbone. *Proc. Natl. Acad. Sci. U.S.A. 101*, 14437−14442.
(36) Karim, C. B., Zhang, Z. W., Howard, E. C., Torgersen, K. D., and Thomas, D. D. (2006) Phosphorylation-dependent conformational switch in spin-labeled phospholamban bound to serca. *J. Mol. Biol. 358*, 1032−1040.
(37) Gustavsson, M., Traaseth, N. J., and Veglia, G. (2012) Probing ground and excited states of phospholamban in model and native lipid membranes by magic angle spinning NMR spectroscopy. *Biochim. Biophys. Acta 1818*, 146−153.
(38) Zamoon, J., Mascioni, A., Thomas, D. D., and Veglia, G. (2003) NMR solution structure and topological orientation of monomeric phospholamban in dodecylphosphocholine micelles. *Biophys. J. 85*, 2589−2598.
(39) Shi, L., Traaseth, N. J., Verardi, R., Gustavsson, M., Gao, J. L., and Veglia, G. (2011) Paramagnetic-based NMR restraints lift residual dipolar coupling degeneracy in multidomain detergent-solubilized membrane proteins. *J. Am. Chem. Soc. 133*, 2232−2241.
(40) Traaseth, N. J., Shi, L., Verardi, R., Mullen, D. G., Barany, G., and Veglia, G. (2009) Structure and topology of monomeric phospholamban in lipid membranes determined by a hybrid solution and solid-state NMR approach. *Proc. Natl. Acad. Sci. U.S.A. 106*, 10165−10170.
(41) Shi, L., Traaseth, N. J., Verardi, R., Cembran, A., Gao, J. L., and Veglia, G. (2009) A refinement protocol to determine structure, topology, and depth of insertion of membrane proteins using hybrid solution and solid-state NMR restraints. *J. Biomol. NMR 44*, 195−205.
(42) Masterson, L. R., Yu, T., Shi, L., Wang, Y., Gustavsson, M., Mueller, M. M., and Veglia, G. (2011) Camp-dependent protein kinase a selects the excited state of the membrane substrate phospholamban. *J. Mol. Biol. 412*, 155−164.
(43) Zamoon, J., Nitu, F., Karim, C., Thomas, D. D., and Veglia, G. (2005) Mapping the interaction surface of a membrane protein: Unveiling the conformational switch of phospholamban in calcium pump regulation. *Proc. Natl. Acad. Sci. U.S.A. 102*, 4747−4752.
(44) Ha, K. N., Traaseth, N. J., Verardi, R., Zamoon, J., Cembran, A., Karim, C. B., Thomas, D. D., and Veglia, G. (2007) Controlling the inhibition of the sarcoplasmic Ca^{2+}-ATPase by tuning phospholamban structural dynamics. *J. Biol. Chem. 282*, 37205−37214.
(45) Traaseth, N. J., Thomas, D. D., and Veglia, G. (2006) Effects of Ser16 phosphorylation on the allosteric transitions of phospholamban/Ca^{2+}-ATPase complex. *J. Mol. Biol. 358*, 1041−1050.
(46) Raake, P. W. J., Tscheschner, H., Reinkober, J., Ritterhoff, J., Katus, H. A., Koch, W. J., and Most, P. (2011) Gene therapy targets in heart failure: The path to translation. *Clin. Pharm. Ther. 90*, 542−553.
(47) Ha, K. N., Gustavsson, M., and Veglia, G. (2012) Tuning the structural coupling between the transmembrane and cytoplasmic domains of phospholamban to control sarcoplasmic reticulum Ca^{2+}-ATPase (serca) function. *J. Muscle Res. Cell Motil. 33*, 485−492.
(48) De Simone, A., Montalvao, R. W., and Vendruscolo, M. (2011) Determination of conformational equilibria in proteins using residual dipolar couplings. *J. Chem. Theory Comput. 7*, 4189−4195.
(49) Montalvao, R. W., De Simone, A., and Vendruscolo, M. (2012) Determination of structural fluctuations of proteins from structure-based calculations of residual dipolar couplings. *J. Biomol. NMR 53*, 281−292.
(50) Buck, B., Zamoon, J., Kirby, T. L., DeSilva, T. M., Karim, C., Thomas, D., and Veglia, G. (2003) Overexpression, purification, and characterization of recombinant Ca-ATPase regulators for high-resolution solution and solid-state NMR studies. *Protein Expression Purif. 30*, 253−261.
(51) Metcalfe, E. E., Traaseth, N. J., and Veglia, G. (2005) Serine 16 phosphorylation induces an order-to-disorder transition in monomeric phospholamban. *Biochemistry 44*, 4386−4396.
(52) Chou, J. J., Gaemers, S., Howder, B., Louis, J. M., and Bax, A. (2001) A simple apparatus for generating stretched polyacrylamide gels, yielding uniform alignment of proteins and detergent micelles. *J. Biomol. NMR 21*, 377−382.
(53) Permi, P., Rosevear, P. R., and Annila, A. (2000) A set of hnco-based experiments for measurement of residual dipolar couplings in N-15, C-13, (h-2)-labeled proteins. *J. Biomol. NMR 17*, 43−54.
(54) Wymore, T., Gao, X. F., and Wong, T. C. (1999) Molecular dynamics simulation of the structure and dynamics of a dodecylphosphocholine micelle in aqueous solution. *J. Mol. Struct. 485*, 195−210.
(55) Hess, B., Kutzner, C., van der Spoel, D., and Lindahl, E. (2008) Gromacs 4: Algorithms for highly efficient, load-balanced, and scalable molecular simulation. *J. Chem. Theory Comput. 4*, 435−447.
(56) De Simone, A., Richter, B., Salvatella, X., and Vendruscolo, M. (2009) Toward an accurate determination of free energy landscapes in solution states of proteins. *J. Am. Chem. Soc. 131*, 3810−3811.
(57) Hornak, V., Abel, R., Okur, A., Strockbine, B., Roitberg, A., and Simmerling, C. (2006) Comparison of multiple Amber force fields and development of improved protein backbone parameters. *Proteins 65*, 712−725.
(58) Best, R. B., and Hummer, G. (2009) Optimized molecular dynamics force fields applied to the helix-coil transition of polypeptides. *J. Phys. Chem. B 113*, 9004−9015.
(59) Lindorff-Larsen, K., Piana, S., Palmo, K., Maragakis, P., Klepeis, J. L., Dror, R. O., and Shaw, D. E. (2010) Improved side-chain torsion potentials for the Amber ff99sb protein force field. *Proteins 78*, 1950−1958.
(60) Tieleman, D. P., van der Spoel, D., and Berendsen, H. J. C. (2000) Molecular dynamics simulations of dodecylphosphocholine micelles at three different aggregate sizes: Micellar structure and chain relaxation. *J. Phys. Chem. B 104*, 6380−6388.
(61) Jorgensen, W. L., Chandrasekhar, J., Madura, J. D., Impey, R. W., and Klein, M. L. (1983) Comparison of simple potential functions for simulating liquid water. *J. Chem. Phys. 79*, 926−935.
(62) Hess, B., Bekker, H., Berendsen, H. J. C., and Fraaije, J. (1997) Lincs: A linear constraint solver for molecular simulations. *J. Comput. Chem. 18*, 1463−1472.
(63) Darden, T., York, D., and Pedersen, L. (1993) Particle mesh Ewald: An n.Log(n) method for ewald sums in large systems. *J. Chem. Phys. 98*, 10089−10092.
(64) Bussi, G., Donadio, D., and Parrinello, M. (2007) Canonical sampling through velocity rescaling. *J. Chem. Phys. 126*, 014101.
(65) Berendsen, H. J. C., Postma, J. P. M., Vangunsteren, W. F., Di Nola, A., and Haak, J. R. (1984) Molecular-dynamics with coupling to an external bath. *J. Chem. Phys. 81*, 3684−3690.
(66) Cavalli, A., Camilloni, C., and Vendruscolo, M. (2013) Molecular dynamics simulations with replica-averaged structural restraints generate structural ensembles according to the maximum entropy principle. *J. Chem. Phys. 138*, 094112.
(67) Pitera, J. W., and Chodera, J. D. (2012) On the use of experimental observations to bias simulated ensembles. *J. Chem. Theory Comput. 8*, 3445−3451.
(68) Roux, B., and Weare, J. (2013) On the statistical equivalence of restrained-ensemble simulations with the maximum entropy method. *J. Chem. Phys. 138*, 084107.
(69) Zhou, Y. P., Cierpicki, T., Jimenez, R. H. F., Lukasik, S. M., Ellena, J. F., Cafiso, D. S., Kadokura, H., Beckwith, J., and Bushweller, J. H. (2008) NMR solution structure of the integral membrane enzyme dsbb: Functional insights into dsbb-catalyzed disulfide bond formation. *Mol. Cell 31*, 896−908.
(70) Camilloni, C., Robustelli, P., De Simone, A., Cavalli, A., and Vendruscolo, M. (2012) Characterization of the conformational equilibrium between the two major substates of RNase a using NMR chemical shifts. *J. Am. Chem. Soc. 134*, 3968−3971.

(71) Karim, C. B., Marquardt, C. G., Stamm, J. D., Barany, G., and Thomas, D. D. (2000) Synthetic null-cysteine phospholamban analogue and the corresponding transmembrane domain inhibit the Ca-ATPase. *Biochemistry 39*, 10892−10897.
(72) Clore, G. M., and Schwieters, C. D. (2004) Amplitudes of protein backbone dynamics and correlated motions in a small α/β protein: Correspondence of dipolar coupling and heteronuclear relaxation measurements. *Biochemistry 43*, 10678−10691.
(73) Clore, G. M., and Schwieters, C. D. (2004) How much backbone motion in ubiquitin is required to account for dipolar coupling data measured in multiple alignment media as assessed by independent cross-validation? *J. Am. Chem. Soc. 126*, 2923−2938.
(74) Bouvignies, G., Markwick, P., Bruschweiler, R., and Blackledge, M. (2006) Simultaneous determination of protein backbone structure and dynamics from residual dipolar couplings. *J. Am. Chem. Soc. 128*, 15100−15101.
(75) Iwahara, J., Zweckstetter, M., and Clore, G. M. (2006) NMR structural and kinetic characterization of a homeodomain diffusing and hopping on nonspecific DNA. *Proc. Natl. Acad. Sci. U.S.A. 103*, 15062−15067.
(76) Lange, O. F., Lakomek, N. A., Fares, C., Schroder, G. F., Walter, K. F. A., Becker, S., Meiler, J., Grubmuller, H., Griesinger, C., and de Groot, B. L. (2008) Recognition dynamics up to microseconds revealed from an RDC-derived ubiquitin ensemble in solution. *Science 320*, 1471−1475.
(77) Fenwick, R. B., Esteban-Martin, S., Richter, B., Lee, D., Walter, K. F. A., Milovanovic, D., Becker, S., Lakomek, N. A., Griesinger, C., and Salvatella, X. (2011) Weak long-range correlated motions in a surface patch of ubiquitin involved in molecular recognition. *J. Am. Chem. Soc. 133*, 10336−10339.
(78) Huang, J. R., and Grzesiek, S. (2010) Ensemble calculations of unstructured proteins constrained by RDC and PRE data: A case study of urea-denatured ubiquitin. *J. Am. Chem. Soc. 132*, 694−705.
(79) Zweckstetter, M., and Bax, A. (2000) Prediction of sterically induced alignment in a dilute liquid crystalline phase: Aid to protein structure determination by NMR. *J. Am. Chem. Soc. 122*, 3791−3792.
(80) Losonczi, J. A., Andrec, M., Fischer, M. W. F., and Prestegard, J. H. (1999) Order matrix analysis of residual dipolar couplings using singular value decomposition. *J. Magn. Reson. 138*, 334−342.
(81) Oxenoid, K., and Chou, J. J. (2005) The structure of phospholamban pentamer reveals a channel-like architecture in membranes. *Proc. Natl. Acad. Sci. U.S.A. 102*, 10870−10875.
(82) Camilloni, C., De Simone, A., Vranken, W. F., and Vendruscolo, M. (2012) Determination of secondary structure populations in disordered states of proteins using nuclear magnetic resonance chemical shifts. *Biochemistry 51*, 2224−2231.